The complicating role of pnictogen bond formation in the solution-phase and solid-state structures of the heavier pnictogen atranes.

Journal:	*Dalton Transactions*
Manuscript ID	DT-ART-05-2022-001377.R1
Article Type:	Paper
Date Submitted by the Author:	30-Jun-2022
Complete List of Authors:	Moaven, Shiva; Texas Tech University, Chemistry and Biochemistry; University of Oregon, Chemistry and Biochemistry Villanueva, Olivia; Texas Tech University, Chemistry Unruh, Daniel; Texas Tech University, Chemistry and Biochemistry Cozzolino, Anthony; Texas Tech University, Department of Chemistry and Biochemistry

The complicating role of pnictogen bond formation in the solution-phase and solid-state structures of the heavier pnictogen atranes.

Shiva Moaven,† Olivia H. Villanueva,† Daniel K. Unruh, and Anthony F. Cozzolino*

The structure of the simplest stibatrane has been a mystery since it was first prepared in 1966. This study reports the preparation and characterization of two stibatranes from triethanolamine and triisopropanolamine. Solid state structures reveal macrocycles that contain favorable inter- and intramolecular pnictogen bonds. Solution studies, corroborated by DFT analysis, reveal an equilibrium mixture assigned to monomer and pnictogen-bonded dimer. This allowed for the determination of an enthalpy associated with pnictogen bond formation of –27 kJ/mol, in line with the supramolecular nature of these interactions.

Introduction

Atranes are tricyclic molecules with a transannular dative bond between the two bridgehead atoms that generates three 5-membered rings (Fig. 1). A proatrane lacks the transannular bond. The atrane chemistry of many different elements, including transition metals and main group elements,[1–3] has been known for quite some time and their application in a variety of chemical transformations as a reagent or catalyst has been explored.[2,4]
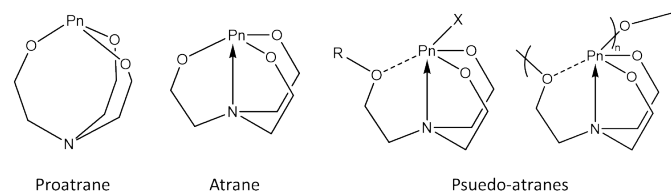

Fig. 1. Depiction of a proatrane (left), atrane (middle), and psuedo-atranes (right). Pn = P, As, Sb, or Bi.

Pnictogen (Pn) atrane chemistry has been mainly limited to P and As. Verkade demonstrated the formation of pro-phosphatrane by treating triethanolamine with tris(dimethylamino)phosphine. Once the prophosphatrane compound was isolated it was shown how the structure could be transformed into phosphatrane using chemical methods such as the oxidation to the phosphine oxide.[5] In 2003, Whitmire reported the bismuth congener. In the crystal structure, the atrane cage ring-opens (partially) at one of the Bi–O bonds to form a short bond with a neighbouring Bi atom resulting in a *pseudo-atrane* (Fig. 1). This propagates in one dimension to form a ladder polymer that is supplemented with additional Bi···O interactions.[6] The material was not found to be soluble in organic solvents and a previous preparation of the materials indicated hydrolysis occurs when exposed to water.[7]

The pnictogen(III) structures appear to range from proatrane for the smallest pnictogens, to a ring-opened pseudo-atrane for bismuth. It seems possible that a molecular stibatrane would fill the gap. Attempts to isolate and characterize the simplest stibatrane from the reaction of antimony(III) sources with triethanolamine have not been successful.[8–11] In the original claim by Müller, the product was described as a white, sublimable substance, but no additional characterization was provided.[8] Another report detailed an attempt to use Sb(OEt)$_3$ as an antimony source, but the product was not structurally characterized.[12] In a more recent attempt, triethanolamine was treated with SbF$_3$ followed by three equivalents of sodium methoxide. The resulting product had two Sb–O bonds and one Sb–F bond, the final equivalent of 'HF' was not removed under these conditions.[8–10] The resulting structure was a tricyclic pseudo-atrane with one of the rings formed though a PnB between the Sb and the OH group (Fig. 2).

In 2005 Parkin and co-workers reported the synthesis of a stibatrane compound through treatment of tris(2-hydroxyphenyl)amine with antimony(III) ethoxide. The structure that was identified contained the expected stibatrane engaging in a pnictogen bond (PnB) with one molecule of DMSO (Fig. 2); the first structurally characterized stibatrane.[13] The PnB

bond forms along the extension of one of the primary Sb–O bonds at a distance that is about 12% longer than a typical SbO single bond (2.05 Å).[14] Some distortion away from three-fold symmetry occurs, presumably to accommodate PnB formation.
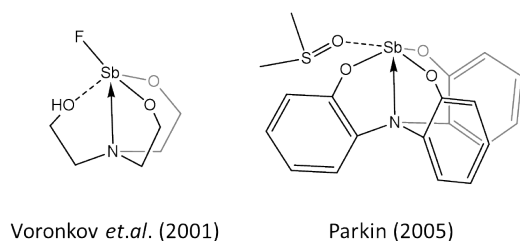

Fig. 2. Most recent structurally characterized product of treatment of SbF₃ and triethanolamine (left). Example of structurally characterized stibatrane (right).[10,15]

It appears that tris(phenoxy)amine compounds do indeed favour the formation of stibatrane compounds. This, coupled with our interest in the pnictogen bonding of antimony cage structures, promoted us to re-examine the possibility of forming stibatranes from the alkyl analogues (Scheme 1).

Results and Discussion

Synthesis
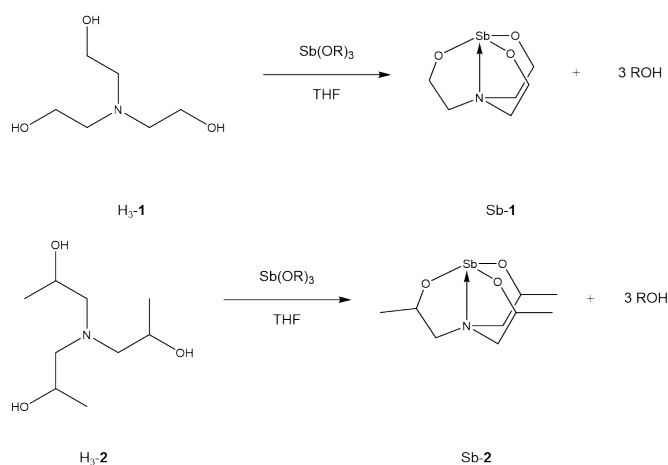
Scheme 1. Reaction routes for preparation of two different purported stibatrane compounds Sb-**1** and Sb-**2**.

For the synthesis of Sb-**1**, anhydrous triethanolamine (H₃-**1**) was treated with antimony(III) *tert*-butoxide in THF (Scheme 1). This resulted in the formation of a white solid that was isolated via filtration. FTIR confirmed the complete disappearance of the O–H stretching band; a deviation from the previously attempted syntheses.[8,10] Although the ¹H NMR in chloroform-*d* did not obviously match with a symmetrical prostibatrane or stibatrane, elemental analysis was consistent with the expected formula. A similar procedure, with a different isolation step, was used for synthesis of Sb-**2**, where anhydrous tri-*iso*-propanolamine (H₃-**2**) was treated with antimony(III) ethoxide in THF. Upon addition, the formation of solids was not

observed. To isolate the product of this reaction, all volatiles were evaporated until a dry white solid was recovered. Again, the disappearance of the O–H stretching band was observed by FTIR which confirmed the complete conversion of tri-*iso*-propanolamine. The ¹H NMR of the compound in chloroform-*d* again was inconsistent with a symmetrical prostibatrane or stibatrane.

Structural Characterization

Single crystals of Sb-**1** were grown by layering a DMSO solution of H₃-**1** on a DCM solution of Sb(OᵗBu)₃. After complete diffusion of both layers, flat square-shaped crystals were isolated. The PXRD of the bulk material was consistent with the predicted pattern, indicating phase-purity (see Figure S1 in the ESI). The crystal structure is shown in Fig. 3 and reveals the formation of a tetrameric macrocycle, denoted (Sb-**1**)₄, instead of the expected monomeric (pro)stibatrane (labelled as Sb-**1** in Scheme 1). Much like the bismuth analogue, the stibatrane appears to have ring-opened. Each Sb forms a primary bond to three oxygen atoms with distances ranging from 2.018(2)-1.976(6). Two Sb–O bonds are within its molecular unit, and one is to a neighbouring molecular unit. In addition, two longer interactions are observed at each Sb atom which are designated as PnBs by virtue of their longer distance and location along the extension of a primary bond. One involves the bridgehead nitrogen at distances of 2.508(2) Å and 2.466(2) Å which corresponds to 113% of the sum of the covalent radii (Σr_cov) of antimony and nitrogen on average. The second PnBs are longer, and presumably weaker, compared to Sb···N, with Sb1···O3 and Sb2···O6 distances of 3.088(3) Å and 3.158(5) Å, respectively, which are on average 146% of Σr_cov. This is in many ways consistent with the structure reported by Voronkov that can be written as Sb-**1**·HF.[10] These motifs appear to indicate that the role of PnB formation in the structure of the heavier analogues of these cages is important. It can be summarized as, PnB formation preferences the antimony and bismuth systems to have the longest interactions arrange opposite a short polar bond. In the solid state, the structures appear to reorganize to achieve this. It could be argued that the 'HF' unit in Sb-**1**·HF proves difficult to remove for similar reasons – its presence facilitates stabilizing PnB interactions. The previously reported bismuth analogue ring-opens to form a pseudo-atrane structure in a manner that is consistent with these arguments.[6] The ability of the heavier pnictogens to form more and stronger PnBs has been explored in a related system and was found to be the result of the interplay of a number of contributions, including size, electronegativity, lone-pair stereochemical inertness, and accessible σ* orbitals.[16]
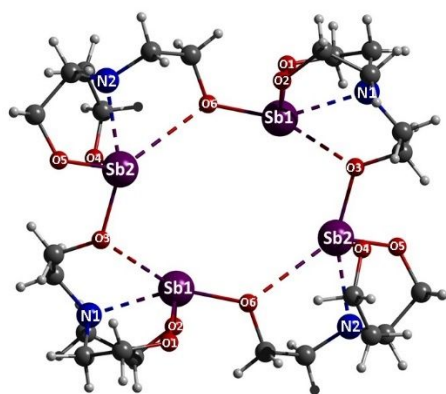
COMMUNICATION

Fig. 3. Ball and stick representation of tetrameric unit of Sb-**1**, (Sb-**1**)$_4$, from crystal structure. PnB interactions are depicted as dashed lines.

Single crystals of the expected Sb-**2** compound, were grown by preparing a saturated solution of the isolated compound in hot DMF and allowing it to cool down to 21 °C. The crystal structure reveals a macrocyclic trimeric, (Sb-**2**)$_3$, and is shown in Fig. 4. Here, it is apparent that using isopropyl groups does not prevent formation of strong intramolecular PnBs between Sb and the N.
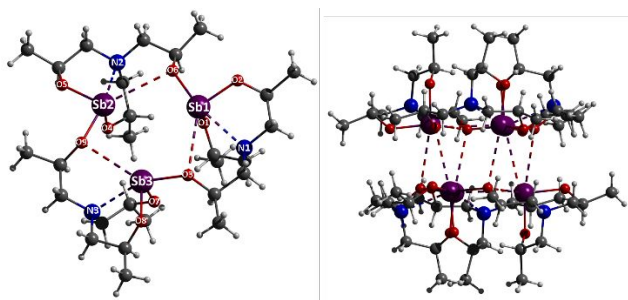

Fig. 4. Ball and stick representation of trimeric unit of *S,S,R*-Sb-**2** from crystal structure (left). Dimer of *S,S,R*-(Sb-**2**)$_3$ and *R,R,S*-(Sb-**2**)$_3$ in solid state (right). PnB interactions depicted as dashed lines.

The enantiopurity of the commercial H$_3$-**2** was not determined and it was assumed all four possible diastereomers (*R,R,R*; *S,S,S*; *R,R,S*; *S,S,R*) were present in the starting material. The single crystal structure of (Sb-**2**)$_3$ is racemic, containing only the *R,R,S* and *S,S,R* enantiomers. The *S,S,R*-(Sb-**2**)$_3$ is shown in Fig. 4. On average, the Sb···N PnB distances are 2.586 Å which is 123% of the Σr_{cov}. Each Sb atom forms medium to weak Sb···O bonds within the cyclic trimer with an average PnB distance of 3.231 Å which is 158% of the Σr_{cov}. The two enantiomers are related by a center of inversion (Fig. 4) and form a dimer that is connected through six Sb···O PnBs with an average distance of 3.223 Å (157% of the Σr_{cov}). In both the *S,S,R*-(Sb-**2**)$_3$ and *R,R,S*-(Sb-**2**)$_3$ macrocycles, the bridging isopropoxy groups are the ones with the unique chiral centres. It is possible that the *S,S,S* or *R,R,R* could form monomeric or psuedo-atranes, but this is unconfirmed as of yet. A powder pattern was collected for the as prepared (Sb-**2**)$_3$ compound (Figure S2). Peaks associated with the single crystal phase can be observed, but the low signal-to-noise ratio suggests the presence of an amorphous

phase which could be due to presence of the *S,S,S* and *R,R,R* isomers of the compounds.

The lack of symmetry in the ^{1}H NMR spectrum of Sb-**1** is consistent with an oligomeric structure like the macrocyclic (Sb-**1**)$_4$ (Figure S4). The hydrogen atoms attached to the carbon adjacent to the O atoms have chemical shifts between 4.0 and 4.2 ppm and their integration value was the same as the signals between 2.5 and 3.1 ppm which correspond to the protons bound to carbons adjacent to the N atoms. Identification of individual proton peaks was not possible as it was determined that the system was also in dynamic equilibrium (vide infra). This contrasts with H$_3$-**1** which contains only two triplets (3.61 ppm and 2.55 ppm in chloroform-*d*). The ^{13}C{^{1}H} NMR (Figure S5) is consistent with the four different chemical environments in the structure that are present in a 2:2:1:1 ratio. Two low intensity broad peaks can be observed that are attributed to the equilibrium partner as discussed later.

Similar to Sb-**1**, once the crystal structure of Sb-**2** was solved, the contribution of an oligomeric species to ^{1}H NMR spectrum became apparent. The ^{1}H NMR of Sb-**2** is shown in Figure S6. Each of the protons adjacent to O atoms have a separate chemical shift between 3.90 ppm and 4.60 ppm. Similarly, the H atoms next to the N atoms have chemical shifts ranging from 2.17-3.21 ppm. The rigidity of the structure caused a slight change in the chemical shift of the methyl group protons too, as multiple methyl protons were found. It must be noted that this NMR is of the bulk material and contains all four isomers along with species in dynamic equilibria. This precludes further interpretation. The ^{13}C{^{1}H} NMR spectrum revealed the presence of a symmetrical system with three resonances and a non-symmetrical system with 9 resonances (Fig. S8).

Solution Equilibria

Given the presence of peaks indicative of a symmetrical structure in the ^{13}C{^{1}H} NMR of Sb-**1**, ^{1}H NMR was re-examined as a function of concentration and temperature. Solutions ranging from 0.01 to 0.04 M were prepared in chloroform-*d* and their ^{1}H spectra were collected at 296, 313, 323, and 333 K. Two sets of changing signals could be followed. One set contains only two resonances (4.07 ppm and 2.84 ppm) and is consistent with the two chemical environments that would be found in a monomeric atrane (or proatrane). These resonances are most apparent at high temperatures and low concentrations, as exemplified in Figures S9-S11. The other sets of resonances, most apparent at high concentrations and low temperatures, are attributed to a less symmetrical system and are consistent with an oligomer as observed in the crystal structure. The relative abundances of monomer and oligomer in each solution were determined by integrating the proton signals in each experiment and monitoring the changes in relative integrated values as a function of temperature.

This provided an opportunity to establish the thermodynamic parameters associated with the dynamic process. Peak areas were measured and extracted from all spectra and fitted according to equations 1 and 2. Equilibrium constants (K_{eq}) were determined for the solutions at constant temperatures.

Contrary to the crystallographic evidence, a linear fit could not be obtained for n=4 (Eq. 1 and 2, Figure S14). The value of n in Eq. 1 and 2 was varied (Figures S12-S14) until a linear fit was obtained. The best fit was obtained for a monomer/dimer equilibrium (n = 2, Figure S12) which is entropically the most feasible. With a series of temperature dependent equilibrium constants, a van't Hoff analysis for the monomer-dimer relationship could be performed. Values of ΔH = −54 kJ·mol^{-1} and ΔS = 140 J·mol^{-1}·K^{-1} (Figure S15 in ESI) were obtained. The positive entropy is consistent with the dimerization process. The enthalpy value is in line with those that have been calculated and experimentally determined for pnictogen bonding.[16,17] Although concentration and temperature changes were observed in the ^{1}H NMR spectra of Sb-**2**; a similar analysis was not performed due to the lack of enantiopurity.

$$n \text{ Sb-}\mathbf{1} \rightleftharpoons (\text{Sb-}\mathbf{1})_n \qquad (1)$$

$$K = [(\text{Sb-}\mathbf{1})_n] / [\text{Sb-}\mathbf{1}]^n \qquad (2)$$

To gain insight into the nature of the monomer and dimer, DFT calculations were performed. The lowest energy structure of the monomer has an atrane geometry; no stable proatrane geometry could be found. The lowest energy geometry is 10.4 kJ·mol^{-1} lower in energy than the second lowest. According to the calculated structure (see Fig 5), the Sb–O distances are 2.045 Å (ave.) and the Sb–N distance is 2.604 Å. These are consistent with the system reported by Parkin (2.084 (ave.) and 2.433 Å, respectively) with small deviations likely due to the pnictogen bonding of DMSO as well as the rigidity of the phenyl rings. A variety of starting points were used in an attempt to model the putative dimer. The lowest energy structure was not a proatrane or pseudo-atrane but is rather a pnictogen-bonded dimer as depicted in Fig 5. Here, the Sb–O distances are 2.048 Å (ave.) for the O atoms not involved in PnBs, and 2.118 Å (ave) for those that are. The Sb-N distances are 2.480 Å and 2.609 Å, and the Sb···O PnB distances are 2.724 and 2.853 Å. The calculated ΔH and ΔS of dimerization (−47.0 kJ·mol^{-1} and 191 J·mol^{-1}·K^{-1}, respectively) are consistent with the experimentally determined values, supporting the model of a pnictogen bonded atrane dimer in solution. Based on the experimental enthalpy, the strength of each PnB can be estimated as 27 kJ·mol^{-1}, in line with the PnB strength evaluated from the enthalpy of sublimation (34 kJ·mol^{-1}) for a related system.[17]
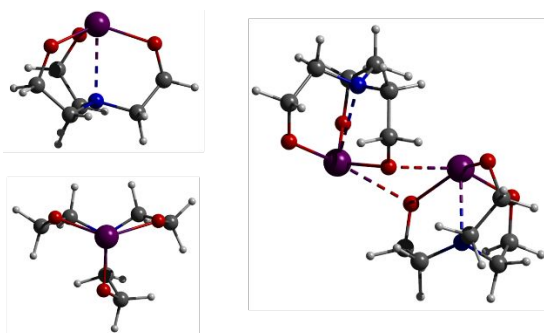

Fig 5. Ball and stick representation of DFT minimized monomer Sb-**1** (left) and lowest energy dimer (Sb-**1**)$_2$ (right). PnB interactions depicted as dashed lines.

Assigning the peaks in the spectra of Sb-**1** allowed for the measurement of the self-diffusion of the two species in solution. Pulsed-field gradient spin-echo (PFGSE) NMR spectroscopy experiments revealed diffusion coefficients of 7.42×10^{-10} m^{2}s^{-1} and 5.51×10^{-10} m^{2}s^{-1} for monomer and dimer, respectively in chloroform-d (Figures S17 and S18). This is consistent with the assignment of the spectra and allows for the estimation of molecular volumes according of the Stokes-Einstein equation. From these, the estimated diameters are 10.8 and 14.6 Å. DFT calculated molecular volumes for the monomer and dimer are 216 and 419 Å^3 which yield diameters of 7.4 and 9.3 Å, respectively. The discrepancy can be attributed to the difference between the solvated and gas phase systems. Given the dissociation that is observed in solution, it seemed feasible that a crystal containing a stibatrane could be grown by sublimation. Attempts to perform this under static vacuum across a temperature gradient resulted in clean sublimation for both Sb-**1** and Sb-**2**. In the case of Sb-**1**, the sublimate only consisted of a microcrystalline powder. The PXRD pattern of the powder was obtained and was found to be distinct from the simulated pattern from the single crystal structure of the tetramer (see Figure S3). The sublimate from Sb-**2** gave larger crystals. Unit cell measurements of sufficiently large crystals revealed a match to the solution grown crystal containing (Sb-**2**)$_3$.

Conclusions

In summary, two new macrocycles were structurally characterized in the pursuit of stibatranes from triethanolamine and tri-*iso*-propanolamine. Pnictogen bonding plays a key role in rationalizing the observed structure. Solution-state studies of these compounds reveal equilibria between monomer and dimer; DFT calculations corroborate these findings and support an atrane structure in solution. An experimental value for the strength of an intermolecular Sb···O bond was determined to be 27 kJ·mol^{-1}. This work supports the idea that PnB formation must be considered as an important structure-directing feature in the design of new trivalent antimony and bismuth compounds.

Acknowledgements

Conflicts of Interest

There are no conflicts to declare

Notes and references

1   J. G. Verkade, *Coord. Chem. Rev.*, 1994, **137**, 233–295.

2   J. G. Verkade, *Acc. Chem. Res.*, 1993, **26**, 483–489.

3   S. N. Adamovich, *Appl. Organomet. Chem.*, 2019, **33**, e4940.

4   M. G. Voronkov and V. P. Baryshok, *Her. Russ. Acad. Sci.*, 2010, **80**, 514–521.

5   D. S. Milbrath and J. G. Verkade, *J. Am. Chem. Soc.*, 1977, **99**, 6607–6613.

6   R. E. Bachman, K. H. Whitmire, J. H. Thurston, A. Gulea, O. Stavila and V. Stavila, *Inorganica Chim. Acta*, 2003, **346**, 249–255.

7   W. T. Miller, *J. Am. Chem. Soc.*, 1940, **62**, 2707–2709.

8   M. G. Voronkov, V. A. Pestunovich, E. A. Zel'bst, A. A. Kashaev, V. S. Fundamenskii, A. I. Albanov, G. A. Kuznetsova and V. P. Baryshok, *Dokl. Chem.*, 2001, **381**, 344–346.

9   V. P. Baryshok and E. A. Zel'bst, *Proc. Univ. Appl. Chem. Biotechnol.*, 2021, **11**, 178–186.

10 M. G. Voronkov, V. A. Pestunovich, A. I. Albanov, G. A. Kuznetsova, É. A. Selbst and V. P. Baryshok, *J. Struct. Chem.*, 2006, **47**, 527–531.

11 R. Müller, *Organomet. Chem. Rev.*, 1966, **1**, 359–377.

12 K. Kumar, S. Dubey, S. N. Misra and R. N. Kapoor, *Egypt J Chem*, 1972, **15**, 267–268.

13 J. M. Tanski, B. V. Kelly and G. Parkin, *Dalton Trans.*, 2005, 2442–2447.

14 B. Cordero, V. Gómez, A. E. Platero-Prats, M. Revés, J. Echeverría, E. Cremades, F. Barragán and S. Alvarez, *Dalton Trans.*, 2008, **0**, 2832–2838.

15 B. V. Kelly, E. C. Weintrob, D. Buccella, J. M. Tanski and G. Parkin, *Inorg. Chem. Commun.*, 2007, **10**, 699–704.

16 H. J. Trubenstein, S. Moaven, M. Vega, D. K. Unruh and A. F. Cozzolino, *New J. Chem.*, 2019, **43**, 14305–14312.

17 S. Moaven, J. Yu, J. Yasin, D. K. Unruh and A. F. Cozzolino, *Inorg. Chem.*, 2017, **56**, 8372–8380.